

Alma Mater Studiorum Università di Bologna
Archivio istituzionale della ricerca

Measurement of soil bulk density and water content with time domain reflectometry: Algorithm implementation and method analysis

This is the submitted version (pre peer-review, preprint) of the following publication:

Published Version:

Bittelli M., Tomei F., Anbazhagan P., Pallapati R.R., Mahajan P., Meisina C., et al. (2021). Measurement of soil bulk density and water content with time domain reflectometry: Algorithm implementation and method analysis. JOURNAL OF HYDROLOGY, 598(July 2021), 1-11 [10.1016/j.jhydrol.2021.126389].

Availability:

This version is available at: <https://hdl.handle.net/11585/829338> since: 2021-08-04

Published:

DOI: <http://doi.org/10.1016/j.jhydrol.2021.126389>

Terms of use:

Some rights reserved. The terms and conditions for the reuse of this version of the manuscript are specified in the publishing policy. For all terms of use and more information see the publisher's website.

This item was downloaded from IRIS Università di Bologna (<https://cris.unibo.it/>).
When citing, please refer to the published version.

(Article begins on next page)

Comparison of Soil Water Content Estimation Equations using Ground Penetrating Radar

Anbazhagan P.¹, Marco Bittelli^{2,*}, Palapati Raghuveer Rao¹ and Puskar Mahajan¹

¹Department of Civil Engineering, Indian Institute of Science, Bangaluru, India

²Department of Agricultural and Food Sciences, University of Bologna, Italy

1

This is a preprint version of:

Bittelli M.; Tomei F.; Anbazhagan P.; Pallapati R.R.; Mahajan P.; Meisina C.; Bordoni M.; Valentino R.

Measurement of soil bulk density and water content with time domain reflectometry: Algorithm implementation and method analysis

which has been published in final form in

JOURNAL OF HYDROLOGY 2021 volume 598 n. 126389

The final published version is available online at: <https://dx.doi.org/10.1016/j.jhydrol.2021.126389>

* Corresponding author. Department of Agricultural and Food Sciences, University of Bologna, Italy, Viale Fanin, 44, 40100 Bologna, Italy. Phone:+39-051-2096644, Fax:+39-051-2096641,E-mail: marco.bittelli@unibo.it; (M. Bittelli)

1 1. Abstract

2 Soil water content (SWC) has an important impact on many fundamental biophysical pro-
3 cesses. The quantification of SWC is necessary for different applications, ranging from large-
4 scale calibration of global-scale climate models to field and catchment scale monitoring in
5 hydrology and agriculture. Many techniques are available today for measuring SWC, ranging
6 from point scale soil water content sensors to global scale, active and passive, microwave satel-
7 lites. Geophysical methods are important methods used for several decades to measure SWC
8 at different scales. Among these methods, Ground Penetrating Radar has been shown to be
9 one the most reliable and promising methods. Soil water content measurement using Ground
10 Penetrating Radar requires the applications of parametric equations that will convert the mea-
11 sured dielectric permittivity to water content. While several tests have been performed to test
12 equations for soil water content sensors such as Time Domain Reflectometry sensors, a few
13 studies have been performed to test different formulae for application to Ground Penetrating
14 Radar. In this study, we compare available formulae for converting dielectric permittivity
15 obtained from detailed laboratory scale measurement of reflected waves using Ground Pene-
16 trating Radar. Four soils covering a wide range of textures were used and the measured soil
17 water contents were compared with values obtained from gravimetric measurements. Results
18 showed that the dielectric mixing model of Roth (1990) provided the best fit both for indi-
19 vidual soil textural classes and for all soils combined, the latter with $RMSE = 0.038 \text{ m}^3 \text{ m}^{-3}$.
20 Sensitivity analysis was then performed to provide detailed information for the most accurate
21 application of the selected model.

22 Keywords: Ground Penetrating Radar, Soil Water Content, Dielectric Mixing Models, Em-

23

24 2. Introduction

25 Soil water content (SWC) is a fundamental property affecting a large variety of processes rel-
 26 evant to hydrology, agricultural sciences, engineering and soil sciences. Over the last decades
 27 many techniques have been developed to measure SWC at different temporal and spatial
 28 scales. Bittelli (2001) provided a review describing the most common methods available for
 29 measuring SWC. Among these methods, geophysical methods have been widely used. Among
 30 geophysical methods, Ground Penetrating Radar (GPR) is a powerful and promising one.
 31 GPR has the advantage of covering larger areas with respect to point-based measurements
 32 typical of soil moisture sensors such as Time Domain Reflectometry (TDR), filling the gap
 33 between point scale and large scale satellite-based measurement. Soil water content can be
 34 obtained by performing different types of analysis and methods using GPR. Huisman et al.
 35 (2003) and Klotzsche et al. (2018) presented reviews about advances in applications of GPR,
 36 for measurement of SWC. In their reviews they discuss the available methods, including contin-
 37 uous multi-offset measurements, off-ground measurements, three-dimensional measurements,
 38 vertical radar profiling, modelling and inverse methods.

39 When the value of soil dielectric permittivity is obtained from GPR, relationships must be
 40 employed to convert permittivity to volumetric SWC. Commonly, the relationships used for
 41 GPR are the ones derived from the calibration of TDR data against SWC data obtained from
 42 gravimetric methods. Since both TDR and GPR are volumetric measurements, during the
 43 calibration measurement of bulk density is necessary to convert the mass-based gravimetric

44 measurement to volume-based soil water content. Many equations were derived over the years.
45 One of the most widely used equations is the one by Topp et al. (1980), which is a third
46 order polynomial. The authors used TDR to measure the dielectric permittivity for a range
47 of granular samples placed in a coaxial transmission line. Ledieu et al. (1986) proposed an
48 equation where the calibration of TDR was performed against gamma-ray attenuation, an
49 accurate technique used for measuring water content. The calibration equation accounted for
50 the change in bulk density of the specimen. Later, Roth et al. (1992) proposed calibration
51 functions for mineral, organic and magnetic soils. These are empirical equations.
52 Roth et al. (1990) proposed a dielectric mixing model based on theoretical considerations. This
53 model includes: 1) the effect of bulk density (by accounting for soil porosity), 2) a geometrical
54 parameter describing the orientation of soil particles with respect to the electric field and
55 3) the values of dielectric permittivity for the solid, liquid and gas phase. While the gas
56 phase permittivity is constant, the solid phase permittivity changes with soil minerals, while
57 the liquid phase permittivity is temperature dependent (assuming constant or narrow-band
58 frequency).

59 The dielectric mixing model of Roth et al. (1990) belongs to the family of the electromagnetic
60 mixing models, which are applied to a large variety of media including snow, ice, liquids and
61 biological materials. One of the most exhaustive description and review about the theory of
62 electromagnetic mixing formula was presented by Sihvola (1999). As pointed out by Sihvola,
63 inhomogeneous mixtures (such as a soil) have properties that are somehow dependent and
64 determined by its constituents but different from the original components. Although the
65 dielectric properties of a mixture are somehow an average of the components permittivities,

66 often the whole character of the dielectric is changed by the mixing process.

67 The relationships currently used for GPR applications were derived from experiments per-
68 formed with the TDR and applied to various studies. Weihermuller et al. (2007) used the
69 Topp et al. (1980) formula to derive water content from GPR. Gerhards et al. (2008) derived
70 SWC from multiple transmitter-and-receiver GPR, employing the Roth et al. (1990) dielectric
71 mixing model.

72 However, there are many differences between TDR and GPR, in terms of frequency of oper-
73 ation, sampling volume, data analysis and interpretation. Therefore there is the need to test
74 the current equations applied to GPR. Only a few studies have been performed. Lambot et
75 al. (2004) estimated SWC directly from GPR, using a soil-specific empirical model (third-
76 order polynomial) similar to Topp's equation. However, their experiment was limited to a
77 sand box with only sand sample as testing material. Steelman and Endres (2010) presented a
78 comparison among petro-physical relationships for application to GPR. They concluded that
79 the general empirical equation by Roth et al. (1992) provided the best fit for the sandy loam
80 soil. When the entire data set was analyzed, they found that the Topp et al. (1980) and Roth
81 et al. (1992) relationships provided the most accurate estimates.

82 However, Steelman and Endres (2010) used permittivity data obtained from GPR using the
83 Common Midpoint (CMP) method. With this method, stacking velocity fields are extracted
84 from multioffset radar soundings at a fixed central location. Yet, CMP-derived velocity esti-
85 mates are generally characterized by low resolution and high uncertainty (Tillard and Dubois,
86 1995; Lambot et al, 2004). The success of the measurements depends on the presence of clearly
87 reflecting layers in the soil. For this reason the calibration equations derived from dielectric

88 permittivity obtained from CMP may be affected by low resolution and high uncertainty.
89 The travel time of the reflected GPR wave depends on the depth of the reflector and the mean
90 dielectric permittivity above the reflector. In general, in field applications the reflectors depth
91 is unknown, therefore alternative techniques are used (Klotzsche et al., 2018). However, for
92 controlled studies on calibration equations, it is more accurate to perform GPR measurements
93 where a reflector is installed at a known depth and derive an accurate travel time, as performed
94 by Lambot et al. (2004), where radar measurements were carried out in controlled laboratory
95 conditions on a tank filled with a disturbed sandy soil.
96 In this study, the performance of various published physical relationships used to obtain soil
97 water content estimates from GPR obtained from a known-depth reflector, were evaluated.
98 Detailed GPR experiments were setup for soils having different texture, bulk density and
99 water content. These variables were controlled and independent gravimetric measurements
100 were used for testing.

101 3. Theory

102 Ground Penetrating Radar reflections occur when there are significant changes in dielectric
103 permittivity. In natural conditions they can be sedimentation layers, groundwater tables,
104 rocks stratification. One of the most common techniques for measuring SWC is based on
105 derivation of dielectric permittivity from travel time analysis.

106 The velocity v [m s^{-1}] of an electromagnetic wave, is affected by the dielectric permittivity ϵ ,
107 and the magnetic permeability μ , as:

$$v = \frac{c}{\sqrt{\mu\epsilon}} \quad (1)$$

108 where c is the speed of light, 2.997×10^8 [m s⁻¹]. From a mechanical standpoint, the velocity
109 v of an electromagnetic wave traveling through a space of length d [m], is given by:

$$v = \frac{2d}{t} \quad (2)$$

110 where t is time [s]. For a reflected wave, the number 2 in front of the length is included because
111 the wave is reflected back to the receiving antenna. For most soils μ_r is equal to 1 (Roth et
112 al., 1992), therefore Eqn. 1 can be written as:

$$v = \frac{c}{\sqrt{\epsilon}} \quad (3)$$

By equating the definitions of velocity:

$$\frac{c}{\sqrt{\epsilon}} = \frac{2d}{t} \quad (4)$$

113 and solving for ϵ :

$$\epsilon = \left(\frac{ct}{2d}\right)^2 \quad (5)$$

114 Equation 5 allows for obtaining the relative dielectric permittivity by measuring the travel
115 time t , since the position of the reflecting plane d and the speed of light c are known. When
116 the material is a composite mixture such a soil, we refer it as bulk dielectric permittivity (ϵ_b).

117 Knowledge of the distance between the antenna and the reflector d , allows for obtaining the
118 travel time and the dielectric permittivity, this method is usually called the *two – way* travel
119 times analysis (Pereira et al., 2005).

120 *3.1. Soil Water Content relationships*

121 *3.1.1. Empirical Equations*

122 The empirical relationship by Topp et al. (1980) is:

$$\theta = -5.3 \times 10^{-2} + 2.92 \times 10^{-2} \epsilon_b - 5.55 \times 10^{-4} \epsilon_b^2 + 4.3 \times 10^{-6} \epsilon_b^3 \quad (6)$$

123 where θ is the volumetric water content ($\text{m}^3 \text{ m}^{-3}$) and ϵ_b is soil bulk dielectric permittivity.

124 The authors fitted the third-order polynomial to TDR data collected in a coaxial transmission
125 line for four soils. They estimated an error for their data of $0.013 \text{ m}^3 \text{ m}^{-3}$.

126 Ledieu et al. (1986) developed an equation obtained from calibrating TDR against SWC data
127 obtained from gamma-ray attenuation. Since dielectric permittivity is density dependent they
128 also included the bulk density. They stated that their procedure and calibration equation had
129 accuracy of less than 1 %. However the experiment was performed only on one sample of sand.

130 The equation proposed is:

$$\theta = 0.1138\sqrt{\epsilon_b} - 0.1758 \quad (7)$$

131 Roth et al. (1992) proposed three different empirical equations for mineral, organic and
132 magnetic soils. The equation for mineral soil is also a third-order polynomial similar to Topp's
133 equation, but with different coefficients and a prediction error of $0.015 \text{ m}^3 \text{ m}^{-3}$:

$$\theta = -7.28 \times 10^{-2} + 4.48 \times 10^{-2} \epsilon_b - 19.5 \times 10^{-4} \epsilon_b^2 + 36.1 \times 10^{-6} \epsilon_b^3 \quad (8)$$

134 *3.1.2. Electromagnetic Mixing Formulas*

135 Electromagnetic mixing formulae relate the value of the individual permittivities of the mixture
 136 components to their volumetric fractions. A widely used class of mixing models are called
 137 power-law models (see Sivhola, 1999, page 166), where a certain power of the permittivity is
 138 averaged over volume weights:

$$\epsilon_b^\beta = f \epsilon_i^\beta + (1 - f) \epsilon_j^\beta \quad (9)$$

139 where ϵ_i and ϵ_j are the generic dielectric permittivities of a two phase systems. In the Birchak
 140 et al., (1974) equation, the parameter β is equal to 1/2. Another known model is the Looyenga
 141 (1965) formula, where β is equal to 1/3.

142 Later Roth et al. (1990), extended the power-law model to compute the bulk dielectric per-
 143 mittivity as a weighted sum of the dielectric permittivity of each soil phase:

$$\epsilon_b = (\phi_s \epsilon_s^\alpha + \theta \epsilon_l^\alpha + \phi_g \epsilon_g^\alpha)^{1/\alpha} \quad (10)$$

144 where ϕ_s , θ and ϕ_g are the solid, liquid and gas phase volumetric fractions. The corresponding
 145 dielectric permittivities are ϵ_s , ϵ_l and ϵ_g , while α is the parameter describing the geometry of
 146 the medium with relation to the applied electric field (Roth et al., 1990). The volumetric solid
 147 fraction can be also written as $\phi_s = (1 - \phi_f)$, where ϕ_f is the porosity and the volumetric

148 fraction of the gas phase as $\phi_g = (\phi_f - \theta)$. Using these relationships and substituting into
 149 eqn. 10, leads to:

$$\theta = \frac{\epsilon_b^\alpha - [(1 - \phi_f)\epsilon_s^\alpha + \phi_f\epsilon_g^\alpha]}{\epsilon_l^\alpha - \epsilon_g^\alpha} \quad (11)$$

150 The liquid phase dielectric permittivity is temperature dependent with:

$$\epsilon_l = 78.54 \times (1 - (4.579 \times 10^{-3} \times \Delta T)) \quad (12)$$

151 where T is temperature in Celsius and $\Delta T = T - 25$. To use this equations, knowledge of
 152 porosity (which can be obtained from measurement of bulk density) and dielectric permittivity
 153 of the solid phase is needed. Porosity is obtained from measured bulk density by:

$$\phi_f = 1 - \frac{\rho_b}{\rho_s} \quad (13)$$

154 where the density of the solid phase (ρ_s) was assumed to be equal to 2.65 g cm^{-3} .

155 The sum of the different volume-weighted permittivities can be extended to include the con-
 156 tribution of organic matter in organic soils, or ice in partially frozen soils (Bittelli et al., 2004).

157 Table 1 provides dielectric permittivity values for different materials (Daniels, 2004). In this
 158 study we used the following values: $\epsilon_s = 4$, ϵ_l was computed with eqn. 12 at $28 \text{ }^\circ\text{C}$, $\epsilon_g = 1.005$
 159 and $\alpha = 0.5$.

160 Overall, the selection of these four models was based on previous results obtained by Steelman
 161 and Endres (2010). They found that the general empirical equation by Roth et al. (1992)
 162 provided the best fit for the sandy loam soil and when the entire data set was analyzed

Table 1: Dielectric permittivity of materials at 100 MHz. From Daniels, 2004.

Material	Dielectric permittivity
Vacuum	1
Air	1.0005
Fresh water	$78.54 \times (1 - 4.579 \times 10^{-3}(T - 25))$
Fresh water ice	3.2
Quartz	4–6
Concrete dry	4–10
Sand Dry	2–6
Sandstone dry	2–5
Soil Dry Clay	4–10
Granite Dry	5
Limestone dry	7

163 using the general empirical expressions, they found that the Topp et al. (1980) and Roth et
 164 al. (1992) relationships provided the most accurate. Regarding the electromagnetic mixing
 165 formulae, Steelman and Endres (2010) found that the Roth et al. (1990) dielectric mixing
 166 model produced better results for the entire data set, but performed only slightly better than
 167 the general empirical relationships.

168 4. Material and Methods

169 Five different soils were used in this study, namely sand, sandy loam, loamy sand and kaolinite
 170 clay. Samples were collected from the Tumkur district, Karnataka, India. The soil samples
 171 were collected from the top 25 cm of soil. The experiments were conducted at laboratory
 172 temperature of 28 °C. This value was used for correcting the dielectric permittivity of the
 173 liquid phase in the dielectric mixing models (eqn.12), which provided a value of $\epsilon_l = 77.46$.
 174 The tested soils were cleaned for presence of organic material like grass, leaves etc. and sieved
 175 with a 2.5 mm size sieve. Figure 1 shows a schematic of the experimental setup, while Figure

176 2 shows two photographs of the experimental setup.

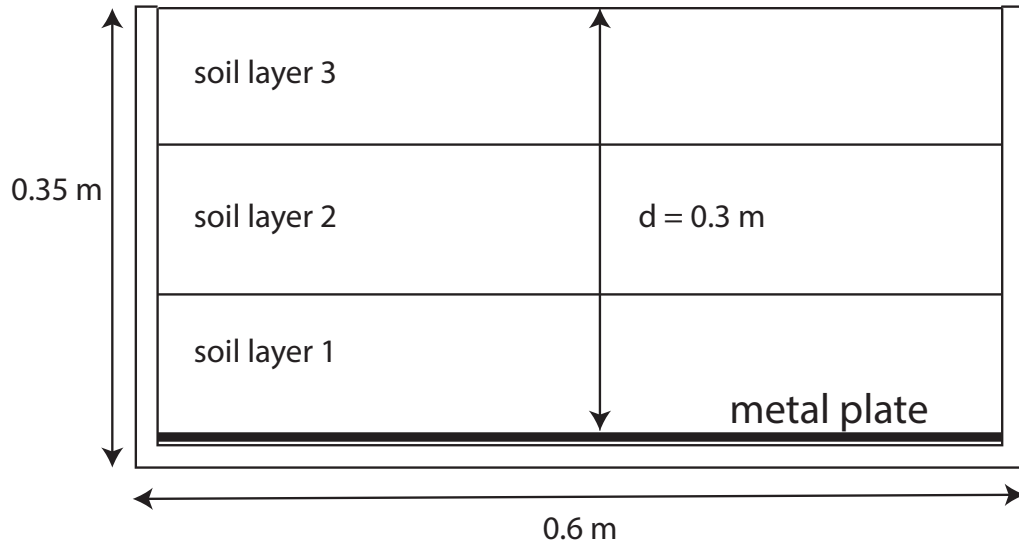


Figure 1: Schematic of the soil plastic tank



Figure 2: Picture of the soil plastic tank and GPR (Mala Inc., 800 MHz).

177 The soil was placed into a plastic tank (with base $0.6 \text{ m} \times 0.4$ and 0.35 m height) for a total
178 volume of $0,072 \text{ m}^3$, with a reflecting metal plate at the bottom. The distance for travel time
179 calculations between the antennas and the reflecting metal plate was $d \simeq 0.3 \text{ m}$. According to
180 the manufacturer (Mala Inc.) the antennas are positioned at the bottom of the GPR, where
181 a plastic lower case of a few mm thickness separate the antennas from the soil. Therefore a

182 value of $d \simeq 0.3$ is the correct physical distance between the antennas and the metal reflector.
183 The distance between the transmitting and receiving antennas is 0.1 m. Materials underneath
184 the metal sheet have no influence on the measured backscattered signal (Lambot et al, 2004).
185 The soil was prepared by adding a fixed amount of water to a specific mass of soil, and mixed
186 to obtain uniform distribution of water. The mixed sample was then placed into the tank and
187 packed to a specific density in three layers of 0.1 meters each, of equal mass. The layers in
188 the figure do not represent different soil types, but the layers used for packing. GPR antenna
189 was then placed on the top of box and readings were taken in time-triggering mode.
190 Subsequently, the soil was removed from the tank and fixed amounts of water were added to
191 increase water content. The same packing procedure was then repeated, therefore everytime
192 the soil was prepared and repacked into the tank, for each SWC measurement. This procedure
193 was followed since it was not possible to increment water content within the tank by either
194 percolation or capillary rise. At the bottom of the tank a reflecting metal plate was positioned
195 for GPR analysis, therefore we could not control the lower boundary condition for percolation
196 or capillary rise with installation of either ceramic or porous plates. Moreover, percolation of
197 water into a tank often results in preferential flows of water along the walls and preferential
198 pathways, resulting in non-homogeneous distributions. For these reasons, the soil was repacked
199 each time for each individual SWC measurement.
200 To verify water content and bulk density values and to test SWC equations, after the GPR
201 measurement was performed, soils samples were collected in metal rings from the center of the
202 tank and independent gravimetric SWC and bulk densities were measured. Although special
203 care was payed to pack the soil at the same density, since the volume of the tank was fairly

204 large, it was not possible to repack the soil at the same densities, therefore variations in bulk
205 densities were recorded during the measurement. These values were used in the equations
206 for estimation of water content, where bulk density (or porosity) was required. Specifically
207 the variations in bulk density ranged from 1.33 to 1.8 g cm⁻³ for sand, from 1.21 to 1.71 g
208 cm⁻³ for sandy loam, from 1.6 to 2.1 g cm⁻³ for loamy sand and from 1.04 to 1.24 g cm⁻³ for
209 kaolinite clay.

210 *4.1. Ground Penetrating Radar measurements*

211 The GPR was a Mala Inc., with an 800 MHz shielded antennas. The setup was the following:
212 time window = 38.8 ns, depth = 0.3 m, sampling frequency = 8230.951172 MHz and antenna
213 separation = 0.1 m. The data were analysed using the software Prism 2 (Radar System Inc.)
214 and Reflex (Sandmeier, 2019). The acquisition was performed in time-based trace triggering
215 mode.

216 Figure 3 shows an example of radargrams showing the reflector depth. The reflection in the
217 upper part of the signal are the typical air and ground wave as shown in Figure 4. The
218 transmitting antenna propagates waves giving rise to an air wave that travel directly from the
219 transmitting to the receiving antenna. Similarly, the propagating wave give rise to the ground
220 wave. The upper part of the radargram shows the air and ground wave.

221 As indicated in Figure 3, the lower change in amplitude indicated by the arrows is the reflection
222 due to the metal plate, determining the travel distance (d) of the wave. Note that in the figure
223 on the left plate the reflection is attenuated (the shade of gray is less intense) with respect to
224 the figure on the right. This is due to a higher water content, determining a higher value of
225 dielectric permittivity, and higher attenuation of the reflected wave. Since the reflector was

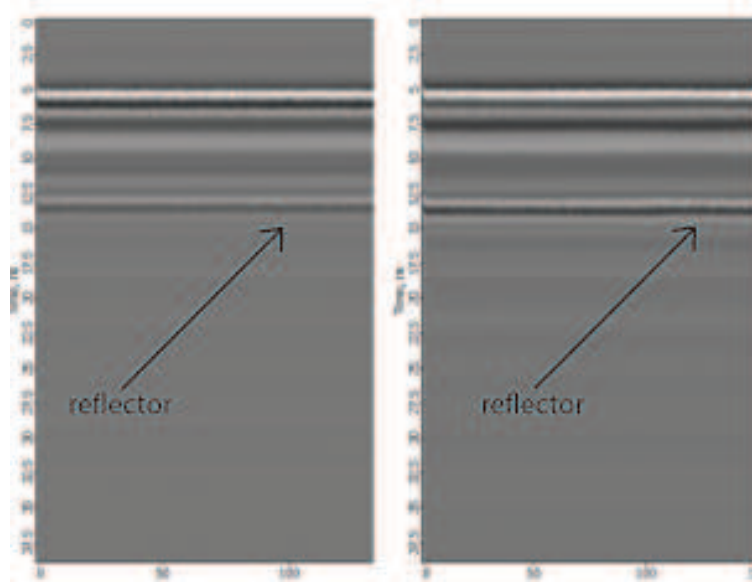


Figure 3: Example of radargrams for two different water contents. The left plate is for a sample at higher water content.

226 fairly close to the antennas (0.3 m), in this study the reflection of the metal plate was always
 227 visible, even at high water content in the kaolinite clay sample.

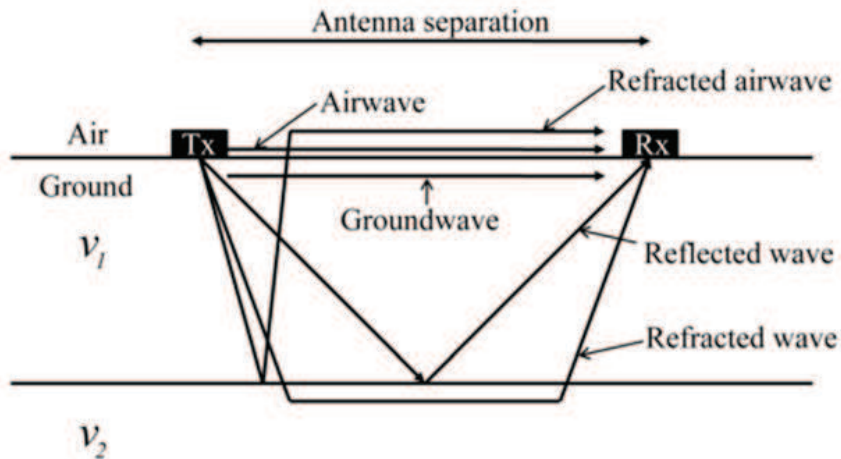


Figure 4: Propagation paths of electromagnetic waves in soils with different layers (Huisman et al., 2003)

228 Indeed, depth penetration is controlled by the dielectric permittivity and electrical conduc-
 229 tivity of the sample. In fine textured soils, in particular in clay soils, the signal can be highly
 230 attenuated. Moreover, in fine textured samples relaxation processes (such as Maxwell-Wagner

231 or double layer polarization) may determine additional dissipation processes (Schwing et al.,
232 2013) and further attenuation of the signal.

233 The procedure to identify the reflections was based on the calibration procedure presented by
234 Pereira et al. (2005). The authors pointed out that one of the main problems related to GPR
235 technology is that the technical information provided by the different companies is practically
236 inexistent. The lack of information for the different parameters for antenna emissions and
237 emitted signal is a serious difficulty for data interpretation. For instance, the authors showed
238 that the rate of drift of the signal was not exactly the same for the three antennas under test,
239 operating at 500, 800 and 1000 MHz. Indeed, the time base of GPR measurements is also not
240 exactly defined and it may exhibit a significant drift due to a temperature difference between
241 the instrument electronics and the air temperature. Accordingly, we increased the warming
242 time of the GPR to 30 minutes to equilibrate with the laboratory temperature. Since the
243 authors used the same GPR manufacturer used in this study (Mala Inc.), we employ their
244 procedure to identify the time zero parameter.

245 An exact definition of time zero is nearly impossible. It is not a constant value but depends on
246 the surface material type and the antenna set up configuration (Sandmeier, 2019). However,
247 when the physical distance of the reflector and the distance between the antenna are known, it
248 is possible to determine the time zero for the investigated material. An automatic and stable
249 static correction (definition of time zero) may be done either on the first negative, first zero
250 crossing or first positive peak (Sandmeier, 2019). Pereira et al. (2005) suggested to use the
251 first positive peak (Fig. 4 in Pereira et al. (2005)) for the 800 MHz antenna.

252 Figure 5 shows an example of a trace and the identification of the reflection for computation

253 of travel time. The lower plate shows the complete trace acquired during the experiment and
254 the upper plate a zoom over the relevant section. The origin was fixed by starting off at the
255 greatest amplitude value from the first positive semiperiod peak. After obtaining the travel
256 time, the bulk dielectric permittivity was then computed as detailed above.

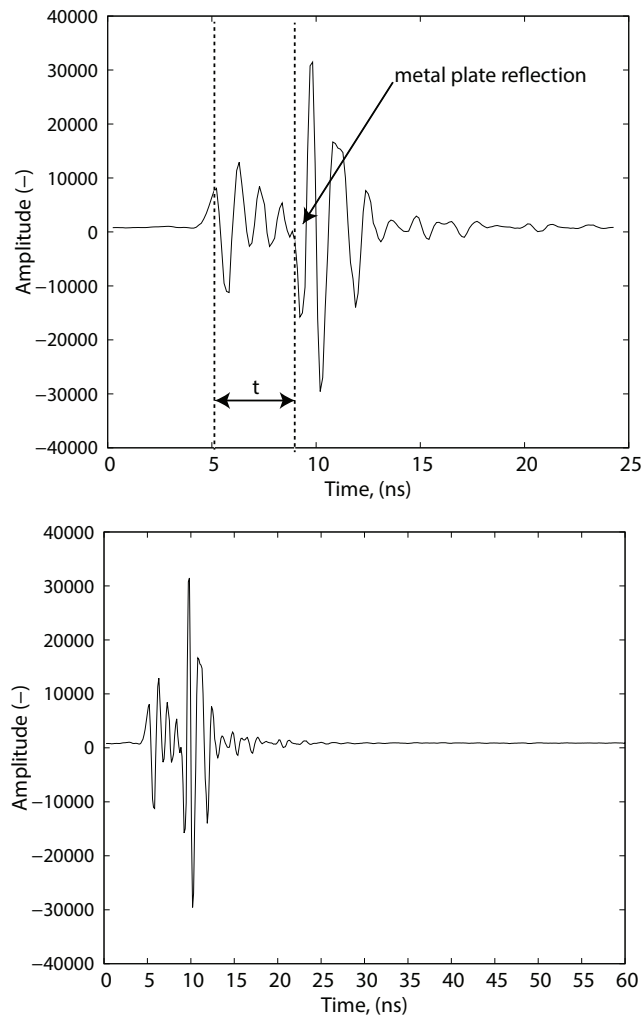


Figure 5: Example of travel time determination on a representative trace

257 *4.2. Error Analysis*

258 The accuracy of the volumetric soil water content estimates was estimated using the Root
 259 Mean Squared Error (RMSE):

$$RMSE = \sqrt{\frac{\sum_{i=1}^N (\theta_{meas} - \theta_{pred})^2}{N}} \quad (14)$$

260 where N is the total number of samples, θ_{meas} [$\text{m}^3 \text{ m}^{-3}$] is the volumetric water content
 261 obtained from gravimetric measurements and θ_{pred} [$\text{m}^3 \text{ m}^{-3}$] is the volumetric water content
 262 predicted by the different equations, and obtained from GPR measurement of bulk dielectric
 263 permittivity.

264 **5. Results and Discussion**

265 The estimated volumetric water contents, θ , obtained from the different equations are pre-
 266 sented in Fig. 6 for the four different textural classes and the RMSE results are presented
 267 in Table 2. The dielectric mixing model of Roth et al. (1990) provided the best fit for the
 268 tested soils, except for the sandy loam. For the sandy loam, the Topp’s and Ledieu’s equations
 269 provided the best fit. When all the data were combined the dielectric mixing model of Roth
 270 et al. (1990) provided the best fit, with RMSE of $0.038 \text{ m}^3 \text{ m}^{-3}$.

Table 2: Root Mean Square Error (RMSE) [$\text{m}^3 \text{ m}^{-3}$] for the four different soil types and all data. DMM stands for dielectric mixing model.

Relationships	sand	sandy loam	loamy sand	kaolinite clay	all data
Topp et al. (1980)	0,024	0,035	0,022	0,033	0,051
Ledieu et al., (1986)	0,023	0,035	0,025	0,030	0,052
Roth et al. (1992)	0,049	0,054	0,015	0,012	0,051
Roth et al. (1990)-DMM	0,022	0,040	0,010	0,010	0,038

271 Figure 6 shows the SWC predicted by the four different equations against the independent
 272 gravimetric SWC. The gravimetric measurements were converted into volume based measure-
 273 ment by multiplying them by the bulk densities. As confirmed by the values of RMSE, it is
 274 also possible to visually see the best fitting of the dielectric mixing model of Roth et al. (1990)
 275 for the indicated textures.

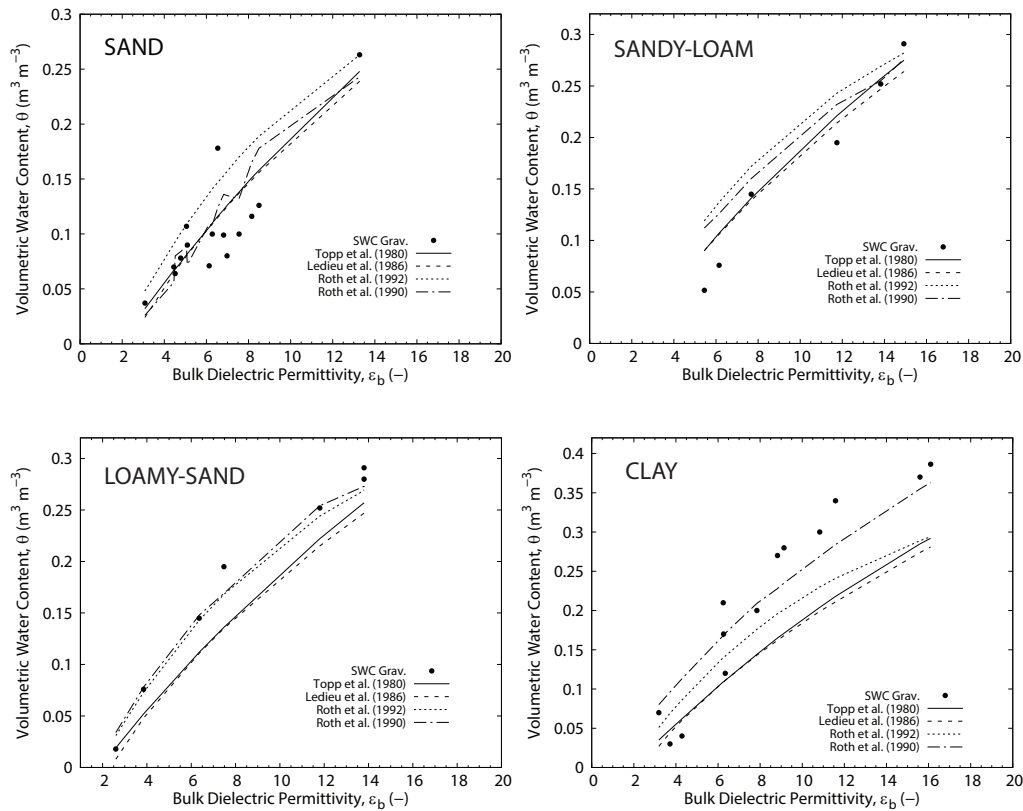


Figure 6: Ground penetrating radar (GPR) permittivity with corresponding volumetric water contents collected for the sand, sandy loam, loamy sand and kaolinite clay textural classes. Points are gravimetric water contents and lines are estimated values for the four different models.

276 Considering the difficulties in achieving uniform packing of wetted soil into a large tank and
 277 the multiple repetitions of the procedure, the scatter of the experimental data is fairly small,
 278 confirming the accuracy of the experimental procedure.

279 Figure 7 shows a scatter plot between the measured volumetric water contents and the esti-

280 mated ones for the different models. The performance of the dielectric mixing model may be
 281 further improved by including different values of solid phase dielectric permittivity based on
 282 mineralogical measurements of the samples.

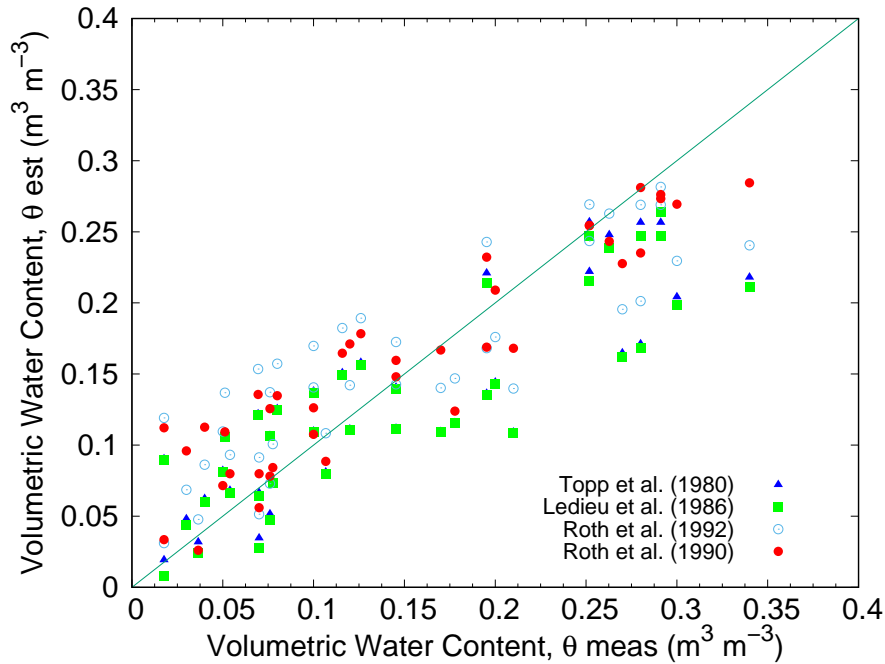


Figure 7: Scatter plot of measured and estimated data for the four soil types

283 Note that the equations that use the value of porosity (or bulk density), such as the dielectric
 284 mixing model of Roth et al. (1990) are not always smooth lines and in particular for sand.
 285 This is due to the varying values of bulk density measured for each independent measurement
 286 of gravimetric SWC.

287 As described above, experimentally was not possible to repack the soil at the exact same values
 288 of bulk density, therefore bulk density was measured every time the soil was repacked. The
 289 ability of estimating SWC as function of porosity is one of the reasons the dielectric mixing
 290 model performed better than the other models.

291 Moreover, the varying bulk densities stress the experimental difficulties of preparing large

292 amount of soil material at uniform water content and density.

293 Using empirical equations, such as the Topp's equation, where estimation of SWC is not den-
294 sity dependent, will lead to inaccurate estimation of SWC since density, in natural conditions,
295 changes with depth. In agricultural conditions, where soil is subject to compaction and soft-
296 ening due to machines and tillage, the changes in bulk density over the growing season are
297 significant, requiring equations that include the possibility of time and space dependent bulk
298 density. For these reasons, there are active lines of research, where direct measurement of bulk
299 density is derived from TDR waveforms, such to obtain both SWC and bulk density from the
300 same waveform measurement (Jung et al., 2013a; Jung et al., 2013b; Curioni et al., 2018).

301 Overall, the dielectric mixing model provides better estimates but it requires knowlegde of soil
302 porosity (or bulk density). We assumed that the liquid phase was in thermal equilibrium with
303 the soil and therefore we used soil temperature for the temperature of the liquid dielectric
304 permittivity. If temperature is not available, default values for ϵ_l at 25°C can be used.
305 However, as discussed below the effects of temperature variations are fairly small. Adjusting
306 the value of ϵ_s would have improved the estimation for the loamy sand soil as well, however
307 we did not want to use ϵ_s as an fitting parameter.

308 These results are consistent with the work of Gerhards et al. (2008), where they derived
309 accurate SWC from GPR using a multiple transmitter-and-receiver setup, and employing the
310 dielectrid mixing model of Roth et al. (1990). As pointed out by Sivhola (1999) the use of
311 dielectric mixing models is preferable with respect to the use of empirical equations since they
312 allow for incorporating dielectric properties of constituent materials and theirvtemperature
313 and frequency dependence. While the major dipole relaxation for water occurs at higher

314 frequency (19 GHz), additional relaxations in soils, such as double layer or Maxwell-Wagner
315 relaxations, may occur in the operational frequencies of GPR, depending on the selected
316 antenna (Olmi and Bittelli, 2015).

317 Another parameter that significantly changes soil water content estimation is the parameter α ,
318 which is discussed in the next section.

319 *5.1. Sensitivity Analysis of the dielectric mixing model*

320 To employ the dielectric mixing model for different media it is important to quantify the
321 effect of the individual parameters on the estimation of water content. As described above the
322 permittivity of the gas phase is constant, the porosity depends on bulk density, the permittivity
323 of the liquid phase is temperature dependent (assuming a constant or narrow band frequency)
324 and the permittivity of the solid phase depends on mineralogy.

325 Figure 8 depicts the variations of volumetric water content as function of permittivity for
326 different values of α . The other parameters are kept fixed with $\epsilon_s = 2$, $\epsilon_l = 77,46$ (at 28 °C),
327 $\epsilon_g = 1.005$ and $\phi_f = 0.547$ (with $\rho_b = 1.2 \text{ g cm}^{-3}$).

328 The parameter α depends on the shape and orientation of the inclusions affecting the depo-
329 larisation factors, as detailed by Sivhola, (1999). The value of 1/2 was used by Birchak et
330 al. (1974) or 1/3 by Looyenga, (1965). Other values can also be selected for the power-law
331 relationship. The domain is $-1 \leq \alpha \leq 1$, where $\alpha = 1$ for plates or other inclusions for which
332 no depolarisation is induced, or when the electric field is parallel to the layering. $\alpha = -1$ if
333 the field is perpendicular to the layering and $\alpha = 0.5$ for isotropic two-phase medium (Roth et
334 al., 1990). Using a non-linear least square minimization algorithm, Roth et al., (1990) found
335 an optimal value of $\alpha = 0.46$ for their experimental data, which is close to 0.5, the value

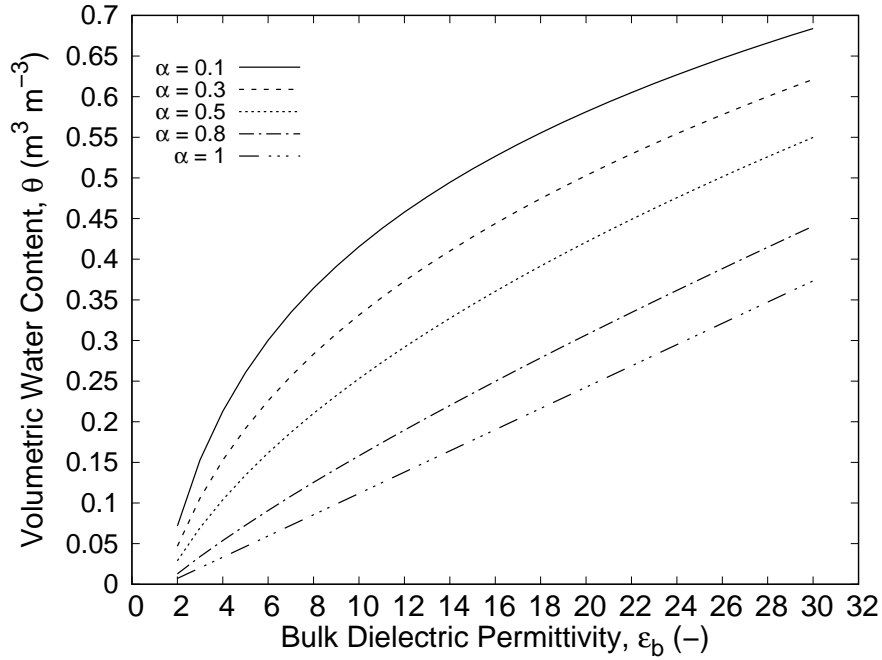


Figure 8: Sensitivity analysis for the parameter α

336 obtained by Birchak et al. (1974) from theoretical reasons. While in this study the dielectric
 337 model was not calibrated and a fixed value of 0.5 was used, α can be modified if information
 338 about the soil layering is available, such as stratifications, sedimentation layers and others.
 339 Alternatively, α can also be used as fitting parameter. At decreasing values of α corresponds
 340 significantly increasing values of θ . Being the relationship non linear the variation depends on
 341 the corresponding values of permittivity.

342 The effect of the solid phase permittivity was also evaluated (Figure 9). The parameters
 343 were kept fixed as for the previous analysis, with $\alpha = 0.5$, and ϵ_s was changed from 2 to 10.
 344 These values are the ones reported in Table 1, for different earth materials. Lower values
 345 are associated to dry sandstone and sand, while higher values are associated to dry clay. The
 346 increase of the solid phase dielectric permittivity determines a decrease in the estimated SWC.
 347 For this parameters set, a change from 2 to 10, determines a decrease in θ of $0.1 \text{ m}^3 \text{ m}^{-3}$.

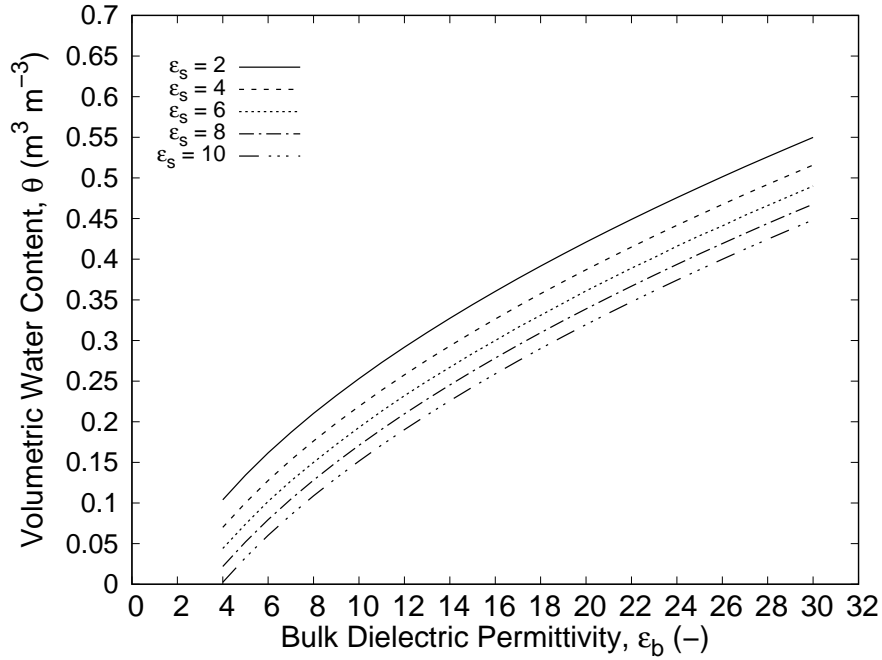


Figure 9: Sensitivity analysis for the parameter ϵ_s

348 This behavior is due to the higher weight given to the the solid phase by an increased ϵ_s in
 349 the weighted volumetric sum, and therefore less weight to the volumetric contribution of the
 350 liquid phase. Also in this case, information regarding the mineralogical composition of the
 351 analyzed media allows for modification of this parameter.

352 The effect of temperature on the liquid phase permittivity, and therefore on θ , is fairly small
 353 with estimated variation in volumetric water contents of about $0.03 \text{ m}^3 \text{ m}^{-3}$ over a temperature
 354 range between 4 and 20 °C. Finally, the effect of porosity on soil water content is about 0.06
 355 $\text{m}^3 \text{ m}^{-3}$ over a variation of ϕ_f between 0.7 and 0.1, with increasing θ with increasing porosity.

356 Considering that in field conditions bulk density can easily range, for instance, between 0.8
 357 and 2.4 g cm^{-3} (corresponding to variations in porosity between 0.7 to $0.09 \text{ m}^3 \text{ m}^{-3}$), the
 358 effect of bulk density is significant on SWC estimation.

359 Overall, the parameters that have a larger effect on estimated SWC with the dielectric mixing

360 model are the exponent α , the solid phase permittivity ϵ_s and porosity ϕ_f . The first two can
361 be used as fixed parameters with values of 0.5 and 4 respectively or used as fitting parameters.
362 Porosity should be measured or obtained from bulk density. In absence of porosity or bulk
363 density data, density can be obtained from TDR waveforms (Jung et al., 2013a, Jung et al.,
364 2013b, Curioni et al., 2018) or from pedotranfer functions by knowledge of textural composition
365 (Rodriguez Lado et al., 2015).

366 6. Conclusions

367 Different relationships to estimate SWC derived from soil permittivities obtained from a two-
368 way GPR analysis data were compared. The GPR data were obtained in a controlled labo-
369 ratory setting using a soil tank with a metal reflector positioned at a known depth, allowing
370 for accurate determination of the soil bulk dielectric permittivity. The data were obtained for
371 four distinct soil textural classes (sand, sandy loam, loamy sand and kaolinite clay) covering
372 a wide range of soil moisture conditions. The physical relationships were empirical and di-
373 electric mixing models. Results showed that the dielectric mixing model of Roth et al. (1990)
374 provided the most accurate estimate of volumetric soil water content, except for sandy loam.
375 The estimation of the dielectric could have been further improved by using the geometric
376 parameter and the dielectric permittivity of the solid phase as fitting parameters. Sensitivity
377 analysis of the dielectric mixing model was performed showing that the geometric parameter
378 α and the dielectric permittivity of the solid phase ϵ_s are the two most sensitive parameters,
379 determining important variations in the estimation of SWC. Based on these results, these two
380 parameters are suggested as fitting parameters to be selected if the model is fitted to data.
381 However, the model can successfully be used without calibration as presented in this study,
382 by using $\alpha = 0.5$ (as also suggested by the authors) and $\epsilon_s = 4$, which is an average value
383 for soil minerals. We suggest to employ the dielectric mixing model of Roth et al. (1990) for
384 estimation of SWC from dielectric permittivity obtained with GPR.

385 7. Acknowledgment

386 This study was funded by: Project Scheme for Promotion of Academic and Research Collab-
387 oration (SPARC). A Government of India Initiative. Project Title: Prediction of Soil Hydro
388 Agricultural Properties using Ground Penetrating Radar for Improving Agricultural Practice
389 (Proposal ID: 375). Responsible: Prof. Anbazhagan P., Department of Civil Engineering,
390 Indian Institute of Science, Bangaluru, India.

391 References

392 Bittelli M., M. Flury and K. Roth 2004. Use of Dielectric Spectroscopy to Estimate Ice Content
393 in Frozen Porous Media. *Water Resour. Res.*,40,W04212,DOI:10.1029/2003WR002343.

394 Bittelli M. 2011 Measuring Soil Water Content: A Review. *Hort. Tech.* , 48, 1-15.

395 Birchak, J.R, L.G. Gardner, J.W. Hipp and J.M. Victor 1974. High dielectric constant mi-
396 crowave probes for sensing soil moisture, *Proceedings of the IEEE*, 62,93-98.

397 Curioni, G., Chapman, D. N., Pring, L. J., Royal, A. C. D., and Metje, N. 2018. Extending
398 TDR capability for Measuring Soil Density and Water Content for Field Condition Moni-
399 toring. *Geotech. J.*, 144(2), 1-15.

400 Daniels, D.J. 2004. *Ground Penetrating Radar*, The Institution of Electrical Engineers, ISBN:
401 O86341360.

402 Gerhards, H., U. Wollschläger, Q. Yu, P. Schiwiek, X. Pan, and K. Roth. 2008. Continu-
403 ous and simultaneous measurement of reflector depth and average soil-water content with
404 multichannel ground-penetrating radar. *Geophysics* 73:J15–J23.

405 Jung S., Drnevich V. P., and Abou Najm M. R. 2013a. New Methodology for Density and
406 Water Content by Time Domain Reflectometry. *Geotech. J.*, 139(5), 659-670.

407 Jung S., Drnevich V. P., and Abou Najm M. R., 2013b. Temperature Corrections for Time
408 Domain Reflectometry Parameters. *Geotech. J.*, 139(5), 671-683.

409 Huisman, J.A., S.S. Hubbard, J.D. Redman, and A.P. 2003. Measuring Soil Water Content
410 with Ground Penetrating Radar: A Review. *Vadose Zone J.*, 2, 476–491.

411 Lambot, S., E.C. Slob, I. van den Bosch, B. Stockbroeckx, and M. Vanclooster. 2004. Modeling
412 of ground-penetrating radar for accurate characterization of subsurface electric properties.
413 IEEE Trans. Geosci. Remote Sens.42:2555–2568.

414 Ledieu, J., Ridder, P. De, Clerck, P. De, and Dautrebande, S. 1986. A method of measuring
415 soil moisture by time-domain reflectometry. J. Hydrol., 88, 319–328.

416 Looyenga H. 1965. Dielectric constants of heterogeneous mixtures, Physica,31, 401-406.

417 Klotzsche, A., F. Jonard, M.C. Looms, J. van der Kruk, and J.A. Huisman 2018. Measuring
418 Soil Water Content with Ground Penetrating Radar: A Decade of Progress Vadose Zone J.
419 17:180052.doi:10.2136/vzj2018.03.0052.

420 Olmi R. and M. Bittelli 2015. Dielectric data analysis: recovering hidden relaxations by fourth-
421 order derivative spectroscopy. IEEE Transactions on Dielectrics and Electrical Insulation,
422 22(6):3334-3340.

423 Pereira, M., Rial, F.I., Lorenzo, H. and Arias, P. 2005. Analysis and calibration of GPR
424 shielded antennas. IEEE 3rd International Workshop on Advanced Ground Penetrating
425 Radar, 2005. IWAGPR 2005. - Delft, The Netherlands. Proceedings of the 3rd Interna-
426 tional Workshop on Advanced Ground Penetrating Radar, 2005. IWAGPR 2005. DOI:
427 10.1109/AGPR.2005.1487878

428 Rodriguez Lado L., M. Rial, T. Taboada and A. Martínez Cortizas. 2015. A Pedotransfer
429 Function to Map Soil Bulk Density from Limited Data. Procedia Environmental Sciences,
430 27, 45-48.

431 Roth, K., R. Schulin, H. Flühler, and W. Attinger. 1990. Calibration of time domain reflectom-
432 etry for water content measurements using a composite dielectric approach. *Water Resour.*
433 *Res.* 26:2267–2273.

434 Roth, C.H., M.A. Malicki, and R. Plagge. 1992. Empirical evaluation of the relationship
435 between soil dielectric constant and volumetric water content as the basis for calibrating
436 soil moisture measurements by TDR. *J. Soil Sci.* 43:1–13.

437 Sandmeier K.J. 2019. Reflex, GPR and seismic data processing software. Version 9.1.
438 <https://www.sandmeier-geo.de/>

439 Schwing, M., Chen Z., Scheuermann A. and Wagner N., 2013. Dielectric properties of a clay soil
440 determined in the frequency range from 1 MHz to 40 GHz. Proc. of the 10th International
441 Conference on electromagnetic Wave Interaction with Water and Moist Substances, ISEMA,
442 Weimar: MFPA, Institute of Material Research and Testing at the Bauhaus University,
443 Weimar (Germany), 242-250.

444 Sihvola, A.H. 1999. Electromagnetic mixing formulas and applications. IEE Electromagn.
445 Waves Ser. 47. Inst. Electr. Eng., London.

446 Steelman, C.M and A.L. Endres. 2011. Comparison of Petrophysical Relationships for
447 Soil Moisture Estimation using GPR Ground Waves Vadose Zone J. 10:270–285,
448 doi:10.2136/vzj2010.0040

449 Tillard, S. and J.-C. Dubois. 1995. Analysis of GPR data: Wave propagation velocity deter-
450 mination. *J. Appl. Geophys.*,33,77–91.

- 451 Topp, G.C., J.L. Davis, and A.P. Annan. 1980. Electromagnetic determination of soil water
452 content: Measurements in coaxial transmission lines. *Water Resour. Res.* 16:574–582.
- 453 Weihermuller, L., J.A. Huisman, S. Lambot, M. Herbst, and H. Vereecken. 2007. Mapping the
454 spatial variation of soil water content at the field scale with different ground penetrating
455 radar techniques. *J. Hydrol.* 340:205–216.